

## Quantitative Theory for Hysteretic Phenomena in CoNi Magnetic Thin Films

R. H. Victora

*Research Laboratories—Diversified Technologies Group, Eastman Kodak Company, Rochester, New York 14650*

(Received 12 November 1986)

For the first time, three-dimensional hysteretic phenomena for a material of moderate coercivity are accurately predicted with use of only microstructural properties as input. The theory includes magnetostatic, crystalline anisotropic, and exchange interactions as suggested by the granular structure. It is found that switching occurs by coherent rotation of individual grains for fields along the perpendicular direction and domain-wall propagation for fields along a longitudinal direction.

PACS numbers: 75.60.Ej, 75.50.Cc, 75.60.Ch, 75.70.-i

Hysteresis is one of the primary manifestations of ferromagnetism, and the consequent experimental and theoretical attention has provided considerable qualitative understanding. Nevertheless, many of the proposed explanations are incomplete or contradictory and it is clear that the development of quantitative theories is of crucial importance for further progress in this field. However, quantitatively accurate predictions from measurable microscopic input are quite difficult for a variety of experimental and theoretical reasons.<sup>1</sup> Accurate characterization of grain boundaries, segregated areas, dislocations, and other irregularities is problematic and the results can vary widely from sample to sample. Many phenomena depend on microscopic nucleation or pinning effects in competition with macroscopic forces. Finally, the magnetostatic interactions and, to a lesser extent, quantum-mechanical exchange make this a many-body problem.

These difficulties have limited the development of quantitative microscopic theories for materials of moderate coercivity such as the CoNi films described here. However, several prominent advances have occurred. Friedberg and Paul<sup>2</sup> have provided a domain-wall pinning theory that predicts the approximate scaling of the coercive force with anisotropy, exchange, and magnetization for a number of metals. Stoner and Wohlfarth<sup>3</sup> suggested a particulate theory that assumed coherent rotations and neglected interparticle interactions; unfortunately, these simplifications typically lead to predicted coercivities 3–10 times greater than experimental ones. The problem of incoherent rotations has been examined in an idealized form by several authors<sup>4</sup>; interactions were successfully treated by Hughes<sup>5</sup> in his two-dimensional calculations for Co-P thin films. Domain nucleation caused by defects or other atomic irregularities has apparently not been considered in quantitative calculations for materials of this coercivity, although its importance in softer materials is commonly appreciated. It is clear that a quantitatively accurate calculation for a general material of moderate coercivity will require development of a theory that provides for all three of these disparate effects: magnetostatic interac-

tions, incoherent rotations, and domain nucleation.

Reported here are accurate first-principles calculations of hysteresis phenomena for two  $\text{Co}_{80}\text{Ni}_{20}$  thin films. All significant input is derived from experimental data other than the hysteresis loops: The precise value of several other input variables is found to be largely irrelevant. The theory includes magnetostatic, exchange, and crystalline anisotropic interactions; a novel provision for domain nucleation and propagation is also included. It is recognized that samples of different composition or structure may present varying behaviors to a changing magnetic field: The importance of the calculation is the demonstration that the underlying physical mechanisms can be identified and that rigorous theoretical predictions can be made despite the complex magnetic structures typical of moderate-coercivity materials.

The two CoNi thin-film samples have been experimentally characterized.<sup>6</sup> They were formed by oblique evaporation and consist of long columnar grains inclined at an angle to the plane of the film<sup>7</sup> (see Fig. 1). Both samples have thicknesses of approximately 1500 Å and angles of inclination of 50° and 60° to the surface normal. Each grain is approximately 200 Å in diameter. The grain boundaries have a significantly different texture than do the grains under electron microscopy and it is probable that they are partly vacuum. Diffraction

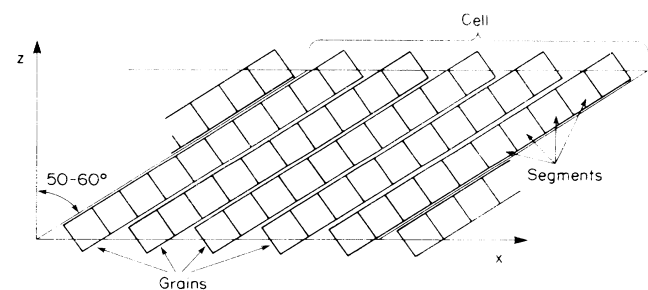


FIG. 1. Simplified description of how cell, grain, and segment boundaries are defined for this calculation. As described in the text, actual grain boundaries used in this calculation are substantially more complex.

studies show the  $c$  axis of the hcp structure to have a wide directional dispersion, which probably tends along the columnar direction.

For calculational purposes the thin film was divided into cells that contain a number of complete grains (see Fig. 1). These cells were linked by periodic boundary conditions and several sizes ranging from  $3 \times 3$  to  $12 \times 10$  grains were used. A variety of grain-boundary patterns, including one taken directly from an electron micrograph, were used; results were found to be insensitive to the precise pattern provided that average grain size, the inclination angle, and the proportion of grain boundary were correct. Each grain was then divided along its major axis into segments such that each segment was approximately cubic.

*Magnetostatic interactions* between all segments are included. For closely neighboring segments (typically within  $1500 \text{ \AA}$ ), the interaction tensor for each pair of segments is calculated by a finite-element integration. For more distant particles, the interaction is included through a mean-field approximation.

The *quantum-mechanical exchange* parameter of bulk  $\text{Co}_{80}\text{Ni}_{20}$  may be approximated by appropriate averaging of the values for pure Co and Ni.<sup>8</sup> This value provides an upper bound for the true value within a grain, which is known to contain dislocations<sup>7</sup> and probably segregations. It is found that calculation results are insensitive to values of the exchange parameter between  $\frac{1}{4}$  and the full bulk value. Thus the calculation is independent of reasonable choice for the exchange parameter and  $\frac{1}{2}$  the bulk value is used:

$$AM_0^2 = 1.32 \times 10^{-6} \text{ ergs/cm.}$$

Quantum-mechanical exchange between grains is neglected because of its expected small value.

The total *anisotropy* of the thin film may be calculated from torque magnetometry. However, the shape contribution to this due to demagnetization fields may also be calculated for each particular arrangement of grains. The difference is, of course, the crystalline anisotropy, which is assumed to be evenly divided between segments and becomes an effective field in the calculations. The  $60^\circ$  sample is found to have negligible net crystalline anisotropy, whereas the  $50^\circ$  grain has crystalline anisotropy  $K = 5 \times 10^5 \text{ ergs/cm}^3$  within grains. This may be compared to the much larger values calculated for the shape anisotropy: approximately  $1.5 \times 10^6 \text{ ergs/cm}^3$  (directed along the columnar axis) for both samples.

The *Landau-Lifshitz-Gilbert equations* are believed to give an adequate description for the time development of the magnetic moment in the case of fixed magnitude.<sup>9,10</sup> This requirement is fulfilled for our small exchange-coupled segments and thus each segment is assigned a magnetization vector  $\mathbf{M}$ , which moves according to

$$\frac{d\mathbf{M}}{dt} = \frac{\gamma}{1+\alpha^2} \mathbf{M} \times \mathbf{H} + \frac{\alpha\gamma}{1+\alpha^2} \hat{\mathbf{M}} \times (\mathbf{M} \times \mathbf{H}).$$

Here  $\mathbf{H}$  includes the applied magnetic field, the magnetostatic interaction fields, the anisotropy fields, and the exchange field. To a large extent, the gyromagnetic ratio  $\gamma$  and damping parameter  $\alpha$  are arbitrary for the nearly static phenomena described here; I have chosen the free-electron value for  $\gamma = 1.76 \times 10^7 \text{ (G s)}^{-1}$  and a value  $\alpha = 1$  for numerical convenience. The temporal integration is conducted by a fourth-order Runge-Kutta<sup>11</sup> scheme with  $\Delta t = 1 \times 10^{-11} \text{ s}$ .

Microscopic *domain nucleation* sites play a major role in magnetization reversal for many materials. Inclusion of these various sites, many of them of unknown nature, would be quite difficult in a calculation of this scale. Instead, my treatment is based on the expectation that the nucleated domain can easily grow until it reaches a grain boundary or the magnetostatic shape effects of the grain become large. Thus, to simulate the effects of domain nucleation within this calculation, single segments within a grain are flipped along the direction of the applied field and this reverse domain is allowed to grow or decay without further intervention. Once equilibrium has been reached and a new external field applied, the process is repeated.

Hysteresis loops for the perpendicular and longitudinal directions of the  $60^\circ$  film are shown in Fig. 2. The agreement with experiment is excellent; in fact, given the approximately 5% level of error in several experimental input variables, the agreement for the perpendicular loop may be regarded as fortuitous. The complementary magnetization data are plotted in Fig. 3. (Magnetization along the transverse direction is small because of the weakness of transversely directed anisotropies.) Figures

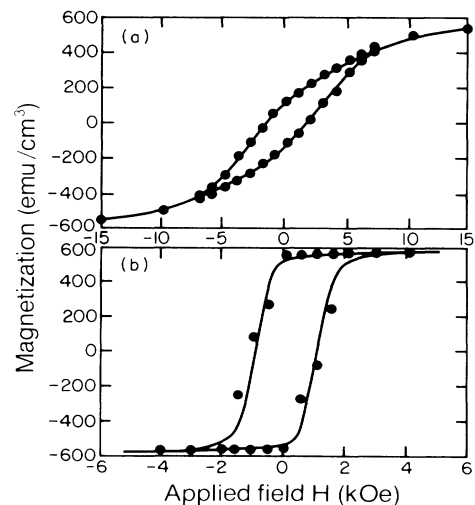


FIG. 2. Experimental (solid line) and theoretical (dots) hysteresis loops. (a) Perpendicular loop for the  $60^\circ$  sample. (b) Longitudinal loop for the  $60^\circ$  sample. (Experimental data taken by L. S. Meichle.)

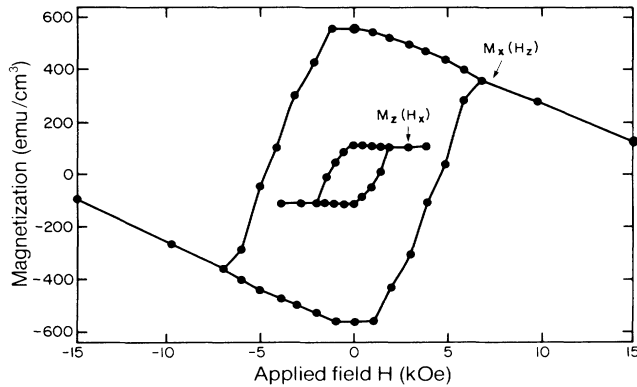


FIG. 3. Theoretical predictions for the magnetization perpendicular to the applied field. Points are connected by straight lines as a guide to the eye.

2 and 3 may be combined to yield the directed macroscopic magnetization for a variety of applied field strengths. Physically it is found that domain nucleation and propagation cause longitudinal hysteresis, with individual grains reversing at different fields and apparently stabilizing their neighbors. On the other hand, domains nucleated in the calculation for the perpendicular loops are typically found to decay rapidly and in no case are they found to have substantial influence on the shape of the loop. In other words, coherent rotation is the dominant effect in perpendicular hysteresis. Finally, hysteresis loops for the  $50^\circ$  sample have also been calculated and shown to have the same excellent level of agreement: Perpendicular coercivity is 2100 Oe for both theory and experiment; longitudinal coercivities are 1350 Oe (experiment) vs 1500 Oe (theory).

In order to examine the transition from coherent rotation to domain nucleation and propagation, the hysteresis loop for a single elongated grain is calculated for a variety of applied field angles. Figure 4(a) shows this "M" shaped curve of coercivity versus applied field angle. It is predicted that nearly coherent rotation occurs for  $\theta < 30^\circ$  and wall propagation for  $\theta > 30^\circ$ . This shape of curve has also been predicted<sup>12</sup> for fanning and curling modes in individual particles; such behavior is precluded in this sample by the shape and very small diameter of the grains. It is to be noted that the absence of magnetostatic interactions with other grains has sharply increased the coercivity of this single grain relative to the film.

The plot of coercivity versus angle of applied field for an entire film is shown in Fig. 4(b). Economy required the use of an abridged sample (most significant is a thickness reduction to 500 Å) and this causes some error, particularly about  $\theta = 0^\circ$ , in the theoretical numbers. Over all, the shape of the experimental plot, particularly the two minimum coercivities, is captured in the theory. The shift of the central minimum away from the hard

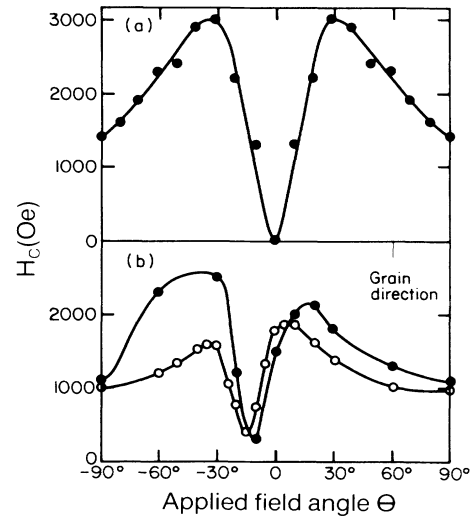


FIG. 4. Coercivity vs angle  $\theta$  of applied field. The applied field direction lies in the  $x$ - $z$  plane and is measured relative to  $z$  axis. (a) Single grain whose major axis is parallel to  $x$  axis. (b)  $60^\circ$  sample. Theoretical points are shown by filled circles; experimental points are shown by open circles. Curves are drawn as a guide to the eye. (Experimental data taken by L. S. Meichle.)

axis ( $\theta = -30^\circ$ ) of the individual grains is found to be the result of a large film demagnetizing field that produces an effective applied field on the grain which is substantially rotated from the true applied field. The most visible discrepancy between experiment and theory occurs about  $\theta = -40^\circ$ . It is noted that at these angles the film demagnetization actually opposes the applied field and makes switching more difficult. [Compare with the low coercivities about  $\theta = 0^\circ$  in Fig. 4(a), where this film demagnetization does not occur.] This means that the reversal of just a few unusual grains will decrease the demagnetizing field and may trigger others to follow in an avalanche. Thus the coercivity would be lowered. Unfortunately, inclusion of this mechanism has not yet been possible on a first-principles basis because of the unknown nature of these postulated grains and their long-range effect.

In conclusion, the first quantitative theory to include domain nucleation, incoherent rotation of grains, and complete magnetostatic interactions has been developed and implemented. The accuracy of this theory is considerable; the few previous attempts to calculate hysteresis loops from microscopic input have usually resulted in errors of a factor of 2-10 in coercivity and substantial difficulties in loop shape. In contrast, this calculation produced longitudinal and perpendicular hysteresis loops that matched experiment to within 10%; the only significant errors occurred at applied-field angles where phenomena are very sensitive to long-range avalanche switching, a possibility not included in this calculation.

The precise values of several input variables such as exchange constant were found to be largely irrelevant; other variables to which the calculation was more sensitive were determined from nonhysteretic experiments such as electron microscopy and torque measurements.

The physical conclusions drawn within the text derive considerable credence from this quantitative accuracy. In particular, it is found that near-perpendicular applied fields produce coherent rotation, whereas more longitudinal fields produce domain nucleation and growth. This latter effect demonstrates the largely unappreciated importance of irregularities spawning new domains in materials of moderate coercivity. The magnetostatic interactions cause two effects: an overall demagnetizing field from the planar shape of the sample, which changes the effective direction and magnitude of the field on a grain, and an overall reduction of coercivity due to partial screening of a grain's shape anisotropy. It is believed that this is the first quantitatively accurate three-dimensional hysteresis calculation for an actual material of moderate coercivity.

I would like to acknowledge experimental data and/or useful discussion provided by A. K. Agarwala, C. F. Brucker, C. Byun, J. S. Gau, L. S. Meichle, and W. E. Yetter. I would also like to thank J. P. Peng for providing independent checks for some of the magnetostatic in-

tegrals.

---

<sup>1</sup>For a more complete description, see W. F. Brown, *Micromagnetics* (Wiley, New York, 1963).

<sup>2</sup>R. Friedberg and D. I. Paul, *Phys. Rev. Lett.* **34**, 1234 (1975).

<sup>3</sup>E. C. Stoner and E. P. Wohlfarth, *Philos. Trans. Roy. Soc. London, Ser. A* **240**, 599 (1948).

<sup>4</sup>See, for example, E. H. Frei, S. Shtrikman, and D. Treves, *Phys. Rev.* **106**, 446 (1957); E. Della Torre, *IEEE Trans. Mag.* **21**, 1423 (1985).

<sup>5</sup>G. F. Hughes, *J. Appl. Phys.* **54**, 5306 (1983).

<sup>6</sup>J.-S. Gau and W. E. Yetter, *J. Appl. Phys.* **61**, 3807 (1987).

<sup>7</sup>Reasons for this common structure are described in, for example, A. G. Dirks and H. J. Leamy, *Thin Solid Films* **47**, 219 (1977); S. Lichter and J. Chen, *Phys. Rev. Lett.* **56**, 1396 (1986).

<sup>8</sup>G. Shirane, V. J. Minkiewicz, and R. Nathans, *J. Appl. Phys.* **39**, 383 (1968).

<sup>9</sup>M. Sparks, *Ferromagnetic Relaxation Theory* (McGraw-Hill, New York, 1964).

<sup>10</sup>A. P. Malozemoff and J. C. Slonczewski, *Magnetic Domain Walls in Bubble Materials* (Academic, New York, 1979), p. 30-39.

<sup>11</sup>G. F. Simmons, *Differential Equations* (McGraw-Hill, New York, 1972).

<sup>12</sup>A. Aharoni, *Phys. Status Solidi* **16**, 3 (1966).